

Defining Plasma Polymerization: New Insight Into What We Should Be Measuring

Andrew Michelmore,^{*,†} Christine Charles,[‡] Rod W. Boswell,[‡] Robert D. Short,[†] and Jason D. Whittle[†]

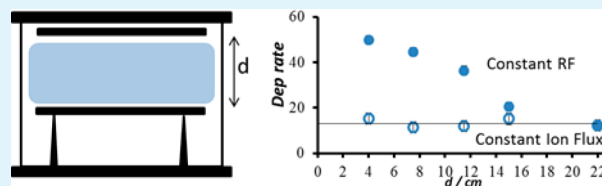
[†]Mawson Institute, University of South Australia, Mawson Lakes Campus, 5095, Adelaide, Australia

[‡]Space Plasma, Power and Propulsion Laboratory, Research School of Physics and Engineering, The Australian National University, ACT 0200, Australia

S Supporting Information

ABSTRACT: External parameters (RF power and precursor flow rate) are typically quoted to define plasma polymerization experiments. Utilizing a parallel-plate electrode reactor with variable geometry, it is shown that these parameters cannot be transferred to reactors with different geometries in order to reproduce plasma polymer films using four precursors. Measurements of ion flux and power coupling efficiency confirm that intrinsic plasma properties vary greatly with reactor geometry at constant applied RF power. It is further demonstrated that controlling intrinsic parameters, in this case the ion flux, offers a more widely applicable method of defining plasma polymerization processes, particularly for saturated and allylic precursors.

KEYWORDS: plasma polymerization, deposition rate, functional retention, ion flux



INTRODUCTION

Plasma polymerization offers a unique method of depositing ultrathin functionalized films onto surfaces for a wide variety of applications, including nanopatterning,^{1,2} nanoparticle coatings,³ controlled release,⁴ and responsive surfaces.^{5,6} The first reported studies of plasma polymerization were in the 1960s,^{7,8} and in 2011 alone over 600 articles describing plasma deposition studies were published. When describing the experimental conditions used, the vast majority of these report the external input parameters RF power (W) and precursor flow rate or pressure (F) at which the experiments were performed as part of the method so that other researchers can replicate. This has been the norm in the field of plasma polymerization for several decades^{e.g. 9–15} This probably stems from the view that the kinetics of traditional polymerization are governed by temperature and concentration¹⁶ and RF power and flow rate are used as proxies for these parameters. The Yasuda parameter (W/FM, where M is the molecular weight) is then used as a scaling factor, giving an indication of the power input per molecule.¹⁷ While this approach may enable deposition kinetics and functional group retention to be calibrated within a single reactor, it offers no insight into the intrinsic plasma processes occurring in the plasma phase or at the substrate, and therefore cannot predict the outcome for reactors of different design. At best, the Yasuda parameter then only provides a “rule-of-thumb” for optimizing plasma polymerization conditions for a given reactor using trial-and-error. For reactors with different geometries, these parameters are near useless. These geometrical differences can include chamber dimensions, electrode type and placement, and even construction materials. An additional complication is that the power coupling efficiency between the RF power and the

plasma is often not taken into account, so the output at the RF power supply may not be representative of the power actually being deposited into the plasma chamber. These gaps in our understanding of plasma polymers have been highlighted in several recent reviews^{18–20} and result in an inability to reproduce results across different laboratories. This has significantly hindered research progress in a wide range of fields. It also inhibits commercial utilization because of scale-up and process control issues.

The question then arises as to which parameters may be routinely measured, and provide a better prediction of plasma polymerization processes. Ions are known to provide energy to substrata in contact with plasma, creating radical sites for neutral species for grafting.²¹ It has also been shown for some monomers that they can contribute mass to the growing deposit.^{22–24} We therefore postulate that ion flux may be a good candidate parameter, as it is either directly or indirectly involved in both deposition routes.^{17,25–29} Additionally, ion flux probes were first developed around 15 years ago³⁰ and have now become relatively cheap and easy to use.

In this study, we used a capacitively coupled reactor with variable interelectrode distance to simulate low pressure RF plasma reactors of different geometry as shown in Figure 1, similar to a previous study.³¹ Deposition experiments were performed using four precursors at a constant pressure of 1 Pa. At the maximum electrode separation of 22 cm, an RF power of 5W was used and the ion flux was measured to be $7.5 \pm 0.35 \times 10^{17}$ ions $m^{-2} s^{-1}$. Then at various smaller separations, two

Received: April 22, 2013

Accepted: June 12, 2013

Published: June 12, 2013

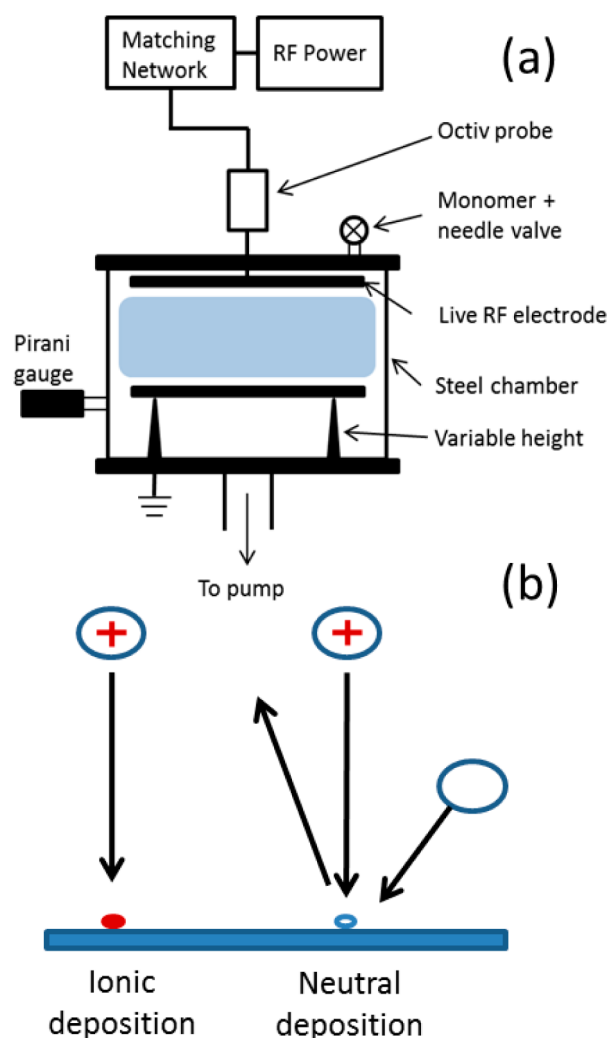


Figure 1. (a) Schematic of the steel plasma reactor used, with variable height earthed electrode, and (b) schematic of the roles of ions in the deposition process.

experiments were performed; one maintaining the RF power at SW, and the other adjusting the RF power to achieve an ion flux of 7.5×10^{17} ions $\text{m}^{-2} \text{s}^{-1}$. The resulting deposition rates and film chemistries are compared.

EXPERIMENTAL SECTION

Materials. The precursor liquids propionic acid, 1-propanol, allyl alcohol, and acrylic acid were purchased from Sigma–Aldrich and used without further purification. Silicon wafers (MMRC Pty. Ltd.) were rinsed in ethanol and acetone before drying under nitrogen.

Plasma Polymerization. The plasma chamber consisted of a 0.25 m steel cylinder with internal diameter 0.3 m. The chamber was evacuated using a rotary pump, with a base pressure of $<2 \times 10^{-2}$ Pa. The flow of monomer into the chamber was controlled with a needle valve. At 1 Pa, the flow rate was measured to be 1.2 sccm for all monomers. RF power at 13.56 MHz was applied to an internal electrode of 0.28 m diameter via a Coaxial power supply (RFG050–13) with a matching network (AMN 150R). The ion flux to the RF electrode was measured using an Impedans OctIV ion flux probe (Impedans, Dublin) placed in series between the matching network and the RF electrode. The probe utilizes the RF electrode to measure the ion flux,³² which for a homogeneous plasma is independent of position.³³ The deposition rate was determined using a Sycon Instruments (USA) Quartz Crystal Microbalance (QCM) using a 6 MHz gold crystal with a diameter of 7 mm placed in the center of the

bottom electrode. Silicon wafer substrates were placed next to the QCM for surface chemistry analysis. The thickness of selected samples was measured by atomic force microscopy using an NT-MDT SPM to confirm the QCM measurements.

X-ray Photoelectron Spectroscopy. XPS spectra were recorded on a SPECS SAGE spectrometer with a Mg $K\alpha$ radiation source operating at 10 kV and 20 mA. The hemispherical analyzer was a Phoibos 150, with an MCD-9 detector. The elements present were identified from a survey spectrum recorded over the binding energy range 0–1000 eV at a pass energy of 100 eV and energy steps of 0.5 eV. High-resolution (0.1 eV steps) spectra were recorded for the C1s photoelectron peaks at a pass energy of 20 eV to identify the chemical binding states. All binding energies were referenced to the aliphatic C1s carbon peak at 285 eV, to compensate for surface charging. The analysis area was circular and 3 mm in diameter. Processing and component fitting of the high-resolution spectra was performed using CasaXPS, with typical full-width-at-half-maxima (fwhm) of 1.5 eV for synthetic peaks.

RESULTS AND DISCUSSION

The deposition rate of 1-propanol and propionic acid plasma are shown in Figure 2. Previously, Barton et al.³³ showed that the kinetics of propionic acid plasma deposition are dominated by ionic processes. It is therefore not surprising that the deposition rate at constant ion flux does not vary as the electrode separation is decreased. However, as the separation is decreased at constant RF power, the deposition rates increase for this compound to around 7.5 cm (after which it falls); later, we show that the plasma density and ion flux increase as electrode separation decrease. It should be noted that as the pressure and molecular weight remain constant, the results at SW correspond to a constant value for the Yasuda parameter for each precursor. At 7.5 cm separation, the deposition rate at SW is increased by a factor of 2.5 compared to the deposition rate at the fixed ion flux of 7.5×10^{17} ions $\text{m}^{-2} \text{s}^{-1}$, demonstrating that the Yasuda parameter cannot predict the deposition rate for different geometries. 1-Propanol shows similar trends, with the deposition rate being constant when the ion flux is kept constant, but increases dramatically for smaller electrode separations at constant RF power.

Allyl groups are known to be able to form oligomers through conventional polymerization, but due to the resonance structure of the allyl group the kinetics are slow and often terminate at short chain lengths.¹⁶ The results in Figure 2 show that radical propagation of allyl alcohol plasmas is unlikely, as the trends are very similar to propionic acid and 1-propanol. For the saturated and allyl precursors used here, the data show the deposition rate is intimately linked with the ion flux, not RF power.

In plasma, polymers of acrylic acid (unsaturated analogue of propionic acid) grow via a combination of ionic deposition and radical polymerization through the carbon double bond.^{34–36} The deposition rate of acrylic acid is typically 3–5 times faster than propionic acid, consistent with our measurements here. Therefore acrylic acid deposition is dominated by neutral/radical chemistry and we might expect the link between deposition rate and ion flux to be less obvious. This is borne out by the results in Figure 2, with the deposition rate at constant ion flux increasing by a factor of around 1.7 from a separation of 22 cm to 7.5 cm after which the rate decreases. Despite this, and surprisingly, the deposition rate correlates better with ion flux than RF power for acrylic acid. Energy transfer via ion impact with substrata can result in surface radical sites being formed to which neutral species can graft,

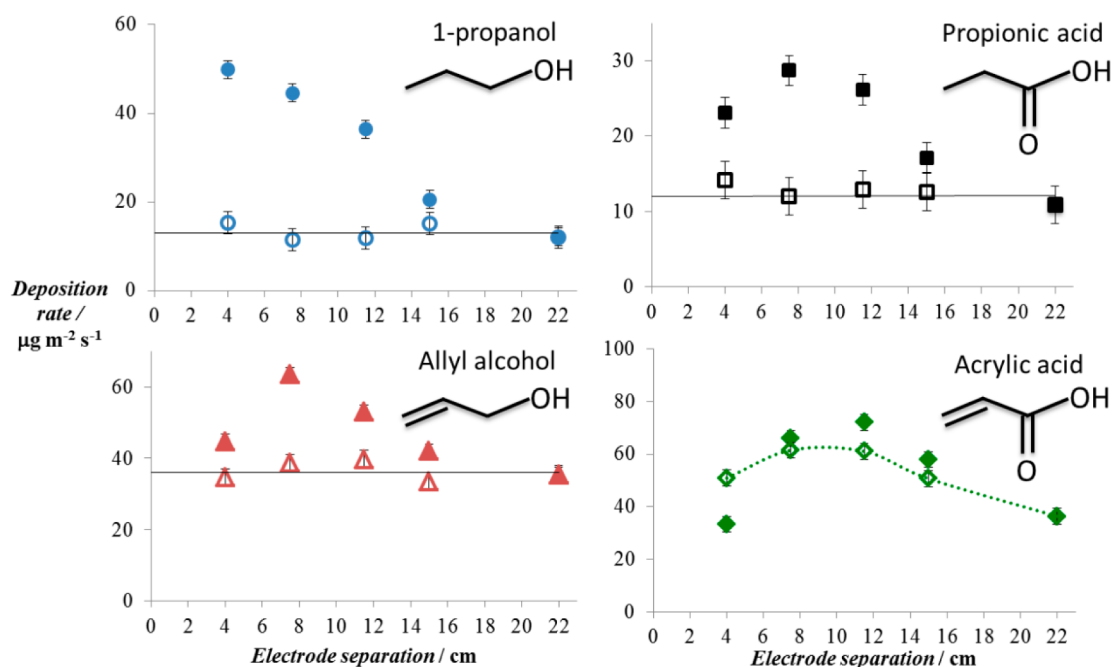


Figure 2. Deposition rate of 4 precursors with electrode separation at 1 Pa at constant RF power of 5W (closed symbols) and constant ion flux of 7.5×10^{17} ions $\text{m}^{-2} \text{s}^{-1}$ (open symbols).

either by radical – radical combination, or radical propagation through carbon double bonds.³⁷ In this case, the link between ion flux and deposition rate will be more complex compared to direct ion adsorption but the ion flux is still an important step. As discussed below, the ion energy increases at small electrode separations, and it has been shown that this also plays a significant role in determining the probability of radical site formation postimpact.³⁸ Awaja et al. showed that increasing the ion energy from 2 to 25 eV increased the surface radical site density by approximately 3 times.³⁹ Similar results have been obtained at 1.5 Pa, and these are presented in the Supporting Information (Figure S1).

Functional group retention is an important parameter in many plasma polymer applications,^{5,6} and is typically measured by X-ray Photoelectron Spectroscopy. The functional group retention of propionic acid remains at around 12% of the C1s envelop at constant ion flux as shown in Figure 3. However at constant RF power, functional group retention decreases with decreasing electrode separation which we attribute to precursor fragmentation in the plasma due to increasing frequency of high energy electron impacts (as a result of electron temperature as discussed below). Functional group retention for acrylic acid decreases slightly from 17% at 22 cm separation to 13.5% at 4 cm at constant ion flux while the results for constant RF power decrease rapidly with decreasing electrode separation. Functional group retention is most likely to be linked to the frequency of high energy electron impacts (with intact compound) and ion–molecule reactions in the plasma phase rather than processes at the substrate.^{40,41} Factors such as monomer residence time, electron density and electron temperature (mostly related to pressure) are therefore likely to affect surface chemistry.

The plasma power (i.e., the RF power actually delivered to the plasma) measured by the OctIV probe is shown in Figure 4. At a constant RF power of 5W, only 3.5W is coupled with the plasma at 22 cm separation. As the separation is decreased the coupling efficiency increases, with 4.7W being deposited into

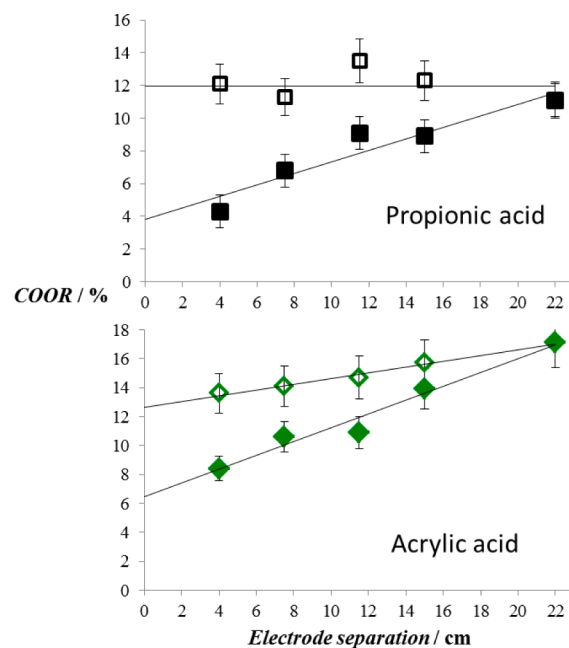


Figure 3. Functional group (COOR) retention for propionic acid and acrylic acid with electrode separation at constant RF power of 5W (closed symbols) and constant ion flux of 7.5×10^{17} ions $\text{m}^{-2} \text{s}^{-1}$ (open symbols).

the plasma at 4 cm separation. This is also evident in the plasma power required to maintain a constant ion flux of 7.5×10^{17} ions $\text{m}^{-2} \text{s}^{-1}$, with the required power decreasing from 3.5W at 22 cm, to 1.3W at 4 cm.

Also shown is the measured ion flux vs electrode separation at constant RF power of 5W. The ion flux increases from 7.5×10^{17} ions $\text{m}^{-2} \text{s}^{-1}$ at 22 cm separation, to around 3×10^{18} ions $\text{m}^{-2} \text{s}^{-1}$ at 4 cm, an increase of 400% over the range of separations tested. It is hardly surprising then that the deposition rates vary at constant RF power. The ion flux to

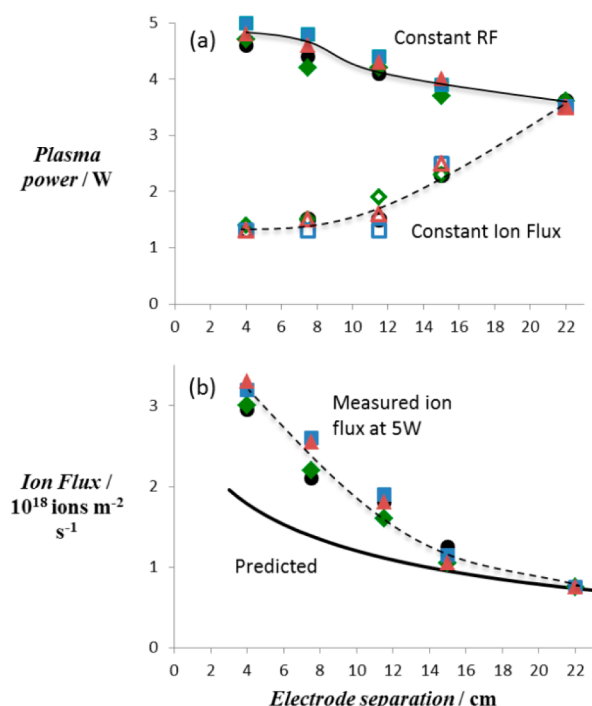


Figure 4. (a) Plasma power vs electrode separation for 4 precursors at constant RF power (closed symbols) and constant ion flux (open symbols); (b) ion flux vs electrode separation at constant RF power. Symbols are the same as Figure 2. The solid line represents the predicted ion flux from a global plasma model at 5 W assuming an electron temperature of 3 eV.

the live electrode calculated as a function of the electrode separation using a previously described power balance in an asymmetric capacitively coupled RF argon discharge^{42,43} is shown by a solid line in Figure 4. The input parameters in the model are a constant RF power of 5 W, a constant and measured matching network resonance factor of 4.5 (the output impedance of the RF generator is 50 Ohm) and a constant electron temperature of 3 eV. The latter was determined by a 1D symmetric capacitive Particle In Cell simulation⁴⁴ and is in agreement with recent experimental data in an asymmetric reactor.⁴⁵ At large separation, the agreement between the model and experimental data is very good; however, as the electrode separation is decreased, the model underestimates the ion flux, by approximately 50% at 4 cm separation. This is probably due to the assumption of a constant electron temperature. Preliminary modeling shows that the electron temperature remains relatively constant at 2.7–3.1 eV for separations between 22 and 11.5 cm, but then increases to around 5 eV at 4 cm. This affects the plasma by increasing the population of high temperature electrons capable of ionizing precursor molecules resulting in greater fragmentation in the plasma phase. A higher electron temperature also implies a higher ion energy ($\sim 5Te$) upon arrival at the substrate surface,⁴⁶ which may affect the sticking probability of ions^{27,47} and sputtering rate of the deposit. The increase in sputtering rate probably accounts for the decrease in deposition rate at small separations observed in Figure 2.

Indeed electron temperature, and therefore ion energy, has an effect on the deposition rate at constant ion flux also.²⁷ The total mass deposited per ion reaching the surface is given by

$$\text{mass/ion} = P_i \Gamma_i m_i - k_s \Gamma_i \quad (1)$$

where Γ_i is the ion flux, m_i is the ion molecular weight, P_i is the sticking probability of the ion, and k_s is the sputtering rate constant. P_i and k_s are both functions of the ion energy. The deposition rate versus separation at 0.5 Pa is given in the Supporting Information (Figure S2). Again, for all four precursors, ion flux is a better predictor of deposition rate than RF power; however, unlike the data at 1 and 1.5 Pa, the relationship is far from linear. Each precursor shows a slight increase in deposition rate from 22 cm to 15 cm, followed by a decrease at smaller separations. This is likely to be due to variations in ion energy, as the electron temperature varies with separation at lower pressures,⁴⁸ in agreement with previous findings.²⁴ It has also been shown recently that energy transfer to the film through ion deposition changes the physical properties of the film through increased cross-linking, affecting parameters such as elastic modulus and solubility.⁴⁹ Therefore, a more complete understanding of the role of ion energy is required in order to predict the deposition rate for reactors of different geometries. This includes the probabilities of sticking and sputtering as a function of ion energy.

CONCLUSION

In conclusion, these results highlight that for low pressure RF plasmas, measuring an external parameter such as RF power does not provide a useful measure of the intrinsic plasma parameters (ion flux, electron temperature, ion energy, etc.) and these change dramatically with reactor geometry (dimensions, materials, electrode type and placement). Therefore, simple power/flow rate measurements offer little guidance in the way of being able to reproduce films in other reactors. The results presented here indicate that ion flux is a better predictor of deposition rate and functional group retention than the often quoted RF power. The correlation with 1-propanol, propionic acid, and allyl alcohol deposition is very strong, as expected with ion adsorption being the dominant mechanism of deposition. The correlation is less convincing for acrylic acid, which may also deposit via radical propagation, but is still an improvement compared to RF power. Functional group retention also remains relatively constant at constant ion flux compared to constant RF power, with this being attributed to plasma phase parameters such as electron temperature and plasma density.

Although this investigation is concerned with low pressure, continuous wave plasma, it is expected that the results will be instructive for other types of plasma. For example, pulsed plasma and downstream processing may also benefit from this type of processing control. For these cases, it is also expected that ion energy will play a role in determining the sticking probability and sputtering rate of ions.

ASSOCIATED CONTENT

Supporting Information

Deposition rate vs electrode separation at constant ion flux and constant power at 0.5 and 1.5 Pa. This material is available free of charge via the Internet at <http://pubs.acs.org>.

AUTHOR INFORMATION

Corresponding Author

*E-mail: andrew.michelmore@unisa.edu.au.

Notes

The authors declare no competing financial interest.

REFERENCES

- (1) Bretagnol, F.; Valsesia, A.; Sasaki, T.; Ceccone, G.; Colpo, P.; Rossi, F. *Adv. Mater.* **2007**, *19*, 1947–1950.
- (2) Muir, B. W.; Fairbrother, A.; Gengenbach, T. R.; Rovere, F.; Abdo, M. A.; McLean, K. M.; Hartley, P. G. *Adv. Mater.* **2006**, *18*, 3079–3082.
- (3) Shi, D. L.; Guo, Y.; Dong, Z. Y.; Lian, J.; Wang, W.; Liu, G. K.; Wang, L. M.; Ewing, R. C. *Adv. Mater.* **2007**, *19*, 4033–4037.
- (4) Vasilev, K.; Sah, V.; Anselme, K.; Ndi, C.; Mateescu, M.; Dollmann, B.; Martinek, P.; Ys, H.; Ploux, L.; Griesser, H. J. *Nano Lett.* **2010**, *10*, 202–207.
- (5) Singamaneni, S.; McConney, M. E.; LeMieux, M. C.; Jiang, H.; Enlow, J. O.; Bunning, T. J.; Naik, R. R.; Tsukruk, V. V. *Adv. Mater.* **2007**, *19*, 4248–4255.
- (6) Mierczynska, A.; Michelmore, A.; Tripathi, A.; Goreham, R. V.; Sedev, R.; Vasilev, K. *Soft Matter* **2012**, *8*, 8399–8404.
- (7) Goodman, J. J. *Polym. Sci.* **1960**, *44*, 551–552.
- (8) Williams, T.; Hayes, M. W. *Nature* **1966**, *209*, 769–773.
- (9) Griesser, H. J. *Vacuum* **1989**, *39*, 485–488.
- (10) Alexander, M. R.; Duc, T. M. *J. Mater. Chem.* **1998**, *8*, 937–943.
- (11) Barry, J. J. A.; Howard, D.; Shakesheff, K. M.; Howdle, S. M.; Alexander, M. R. *Adv. Mater.* **2006**, *18*, 1406–1410.
- (12) Cho, J.; Denes, F. S.; Timmons, R. B. *Chem. Mater.* **2006**, *18*, 2989–2996.
- (13) Bhattacharyya, D.; Yoon, W.-J.; Berger, P. R.; Timmons, R. B. *Adv. Mater.* **2008**, *20*, 2383–2388.
- (14) Alf, M. E.; Asatekin, A.; Barr, M. C.; Baxamusa, S. H.; Chelawat, H.; Ozaydin-Ince, G.; Petruczuk, C. D.; Sreenivasan, R.; Tenhaeff, W. E.; Trujillo, N. J.; Vaddiraju, S.; Xu, J.; Gleason, K. K. *Adv. Mater.* **2010**, *22*, 1993–2027.
- (15) Lin, P. A.; Sankaran, R. M. *Angew. Chem., Int. Ed.* **2011**, *50*, 10953–10956.
- (16) Flory, P. J. *Principles of Polymer Chemistry*; Cornell University Press: New York, 1953.
- (17) Yasuda, H. K. *Plasma Polymerization*; Academic Press: London, U.K., 1985.
- (18) Zheng, J.; Yang, R.; Xie, L.; Qu, J.; Liu, Y.; Li, X. *Adv. Mater.* **2010**, *22*, 1451–1473.
- (19) Friedrich, J. *Plasma Process. Polym.* **2011**, *8*, 783–802.
- (20) Hou, X.; Zhang, H.; Jiang, L. *Angew. Chem., Int. Ed.* **2012**, *51*, 5296–5307.
- (21) Yasuda, H. K.; Hsu, T. J. *Polym. Sci.: Polym. Chem. Ed.* **1977**, *15*, 81–97.
- (22) Candan, S.; Beck, A. J.; O'Toole, L.; Short, R. D.; Goodyear, A.; Braithwaite, N.; St, J. *Phys. Chem. Chem. Phys.* **1999**, *1*, 3117–3121.
- (23) Beck, A. J.; Candan, S.; Short, R. D.; Goodyear, A.; Braithwaite, N.; St, J. *J. Phys. Chem. B* **2001**, *105*, 5730–5736.
- (24) Michelmore, A.; Bryant, P. M.; Steele, D. A.; Vasilev, K.; Bradley, J. W.; Short, R. D. *Langmuir* **2011**, *27*, 11943–11950.
- (25) Denaro, A. R.; Owens, P. A.; Crawshaw, A. *Eur. Polym. J.* **1968**, *4*, 93–106.
- (26) Westwood, A. R. *Eur. Polym. J.* **1971**, *7*, 363–375.
- (27) Choukurov, A.; Kousal, J.; Slavinska, D.; Biederman, H.; Fuoco, E. R.; Tepavcevic, S.; Saucedo, J.; Hanley, L. *Vacuum* **2004**, *75*, 195–205.
- (28) Martinu, L.; Klemberg-Sapieha, J. E.; Kuttel, O. M.; Raveh, A.; Wertheimer, M. R. *J. Vac. Sci. Technol. A* **1994**, *12*, 1360–1364.
- (29) Lee, K.; Deal, M.; McVittie, J.; Plummer, J.; Saraswat, K. *Proceedings of the IEEE International Interconnect Technology Conference*; IEEE: Piscataway, NJ, 1998; pp 175–177.
- (30) Braithwaite, N.; St, J.; Booth, J. P.; Cunge, G. *Plasma Sources Sci. Technol.* **1996**, *5*, 677–684.
- (31) Sciaratta, V.; Hegemann, D.; Müller, M.; Vohrer, U.; Oehr, C. *Upscaling of Plasma Processes for Carboxyl Functionalization. Plasma Processes and Polymers*; Wiley VCH Verlag GmbH & Co. KGaA: Weinheim, Germany, 2005.
- (32) Sobolewski, M. A. *Appl. Phys. Lett.* **1998**, *72*, 1146–1148.
- (33) Barton, D.; Shard, A. G.; Short, R. D.; Bradley, J. W. *J. Phys. Chem. B* **2005**, *109*, 3207–3211.
- (34) O'Toole, L.; Beck, A. J.; Ameen, A. P.; Jones, F. R.; Short, R. D. *J. Chem. Soc. Faraday Trans.* **1995**, *91*, 3907–3912.
- (35) O'Toole, L.; Beck, A. J.; Short, R. D. *Macromolecules* **1996**, *29*, 5172–5177.
- (36) Michelmore, A.; Gross-Kosche, P.; Al-Bataineh, S. A.; Whittle, J. D.; Short, R. D. *Langmuir* **2013**, *29*, 2595–2601.
- (37) d'Agostino, R.; Palumbo, F. *Plasma Process. Polym.* **2012**, *9*, 844–849.
- (38) Charles, C.; Boswell, R. W. *J. Appl. Phys.* **1997**, *81*, 43–49.
- (39) Awaja, F.; Zheng, S.; James, N.; McKenzie, D. R. *Plasma Process. Polym.* **2012**, *9*, 174–179.
- (40) Barton, D.; Short, R. D.; Fraser, S.; Bradley, J. W. *Chem. Commun.* **2003**, *3*, 348–349.
- (41) Steele, D. A.; Short, R. D.; Brown, P.; Mayhew, C. A. *Plasma Process. Polym.* **2011**, *8*, 287–294.
- (42) Charles, C.; Boswell, R. W. *Plasma Sources Sci. Technol.* **2012**, *21*, 022002.
- (43) Menzies, D.; Gengenbach, T.; Forsythe, J. S.; Birbilis, N.; Johnson, G.; Charles, C.; McFarland, G.; Williams, R. J.; Fong, C.; Leech, P.; McLean, K.; Muir, B. W. *Chem. Commun.* **2012**, *48*, 1907–1909.
- (44) Lafleur, T.; Boswell, R. W.; Booth, J. P. *Phys. Plasmas* **2012**, *19*, 194101.
- (45) Gahan, D.; Daniels, S.; Hayden, C.; O'Sullivan, D.; Hopkins, M. B. *Plasma Sources Sci. Technol.* **2012**, *21*, 015002.
- (46) Lieberman, M. A.; Lichtenberg, A. J. *Principles of Plasma Discharges and Materials Processing*; John Wiley and Sons: Hoboken, NJ, 2005.
- (47) Brookes, P. N.; Fraser, S.; Short, R. D.; Hanley, L.; Fuoco, E.; Roberts, A.; Hutton, S. J. *Electron Spectrosc. Relat. Phenom.* **2001**, *121*, 281–297.
- (48) Takahashi, K.; Charles, C.; Boswell, R.; Lieberman, M. A.; Hatakeyama, R. *J. Phys. D: Appl. Phys.* **2010**, *43*, 162001.
- (49) Michelmore, A.; Steele, D. A.; Robinson, D. E.; Whittle, J. D.; Short, R. D. *Soft Matter* **2013**, *9*, 6167–6175.